Planetary and Space Science 60 (2012) 10–17

Contents lists available at ScienceDirect

Planetary and Space Science

journal homepage: www.elsevier.com/locate/pss

Titan's internal structure and the evolutionary consequences

A.D. Fortes [a,b,*]

[a] Centre for Planetary Sciences at UCL/Birkbeck, Gower Street, London WC1E 6BT, UK
[b] Department of Earth Sciences, University College London, Gower Street, London WC1E 6BT, UK

ARTICLE INFO

Article history:
Received 31 August 2010
Received in revised form
22 April 2011
Accepted 25 April 2011
Available online 19 May 2011

Keywords:
Titan
Satellite interiors
Serpentinization

ABSTRACT

Titan's moment of inertia (MoI), estimated from the quadrupole gravity field measured by the Cassini spacecraft, is 0.342, which has been interpreted as evidence of a partially differentiated internal mass distribution. It is shown here that the observed MoI is equally consistent with a fully differentiated internal structure comprising a shell of water ice overlying a low-density silicate core; depending on the chemistry of Titan's subsurface ocean, the core radius is between 1980 and 2120 km, and its uncompressed density is 2570–2460 kg m^{-3}, suggestive of a hydrated CI carbonaceous chondrite mineralogy. Both the partially differentiated and fully differentiated hydrated core models constrain the deep interior to be several hundred degrees cooler than previously thought. I propose that Titan has a warm wet core below, or buffered at, the high-pressure dehydration temperature of its hydrous constituents, and that many of the gases evolved by thermochemical and radiogenic processes in the core (such as CH_4 and ^{40}Ar, respectively) diffuse into the icy mantle to form clathrate hydrates, which in turn may provide a comparatively impermeable barrier to further diffusion. Hence we should not necessarily expect to see a strong isotopic signature of serpentinization in Titan's atmosphere.

© 2011 Elsevier Ltd. All rights reserved.

1. Introduction

The density of Saturn's giant satellite Titan was determined to within 5% of its currently accepted value more than a century ago (See, 1902). Although there was considerable variation in the measured diameter of Titan (due in part to the large optically dense atmosphere), prior to *in situ* space-craft observations, the bulk density was clearly consistent with a mixture of rocky and icy material (Elliot et al., 1975). Subsequent refinements of Titan's mass and solid-body diameter continued into the era of *in situ* space-craft measurements (Jacobson et al., 2006). However, the mass of Titan alone provides no unique constraint on the density *distribution* in the satellite's interior. Only with the recent determination by the Cassini space-craft of the quadrupole terms in the spherical harmonic expansion of the gravitational potential has it become possible to place constraints on the range of allowed internal structure models. As reported by Iess et al. (2010) the magnitudes of the Stokes' coefficients J_2 and C_{22} are consistent with a globally hydrostatic quadrupole field ($J_2/C_{22} \equiv 10/3$): it is therefore possible to use the Darwin–Radau approximation to obtain the normalized polar moment of inertia factor (e.g., Murray and Dermott, 1999). For the two models fitted to the data, the first being a multi-arc solution (SOL1) and the second being a global solution (SOL2), Iess et al. (2010) obtain $C/MR^2 = 0.3414 \pm 0.0005$ and $C/MR^2 = 0.3419 \pm 0.0010$, respectively. Since the hydrostatic quadrupole coefficients may be overestimated by as much as 5%, then C/MR^2 could be as small as 0.33, although a value nearer 0.34 is preferred. Since Titan is remarkable for its dense N_2 atmosphere and evidence for extensive geologically recent resurfacing, determination of the internal structure is of importance in understanding the body's evolution, and placing this in the context of the other large icy satellites' internal structures.

Many workers have published chemical and thermal evolutionary models for Titan (Reynolds and Cassen, 1979; Lupo and Lewis, 1979; Lupo, 1982; Zharkov et al., 1985; Schubert et al., 1986; Sohl et al., 1995; Grasset et al., 2000; Sohl et al., 2003; Tobie et al., 2005, 2006; Prentice, 2007; Fortes et al., 2007; Grindrod et al., 2008). For the most part, these structures pre-suppose dense rocky cores (silicate densities generally in the range 3300–4000 kg m^{-3}), sometimes with denser metallic inner cores. Thermal models tend to indicate that the core will be hot (>1400 K) and losing heat by convection (Grasset et al., 2000; Tobie et al., 2005, 2006). Such temperatures are above the eutectic melting temperature in the Fe–FeS binary system, and so partial melting and segregation of metallic liquid into an inner core is possible. Broadly, the published models have MoI of 0.30–0.33, although Fortes et al. (2007) proposed a model with a MoI = 0.338 comprising a low-density hydrous rocky core and an ice shell bearing a high-density subsurface ocean. In the latter case, it is necessary to maintain a comparatively cool core (<900 K) in order to prevent water loss from hydrous minerals. Most recently, Castillo-Rogez and Lunine (2010) modelled the thermal evolution of Titan's core, accounting for the onset of dehydration, and concluded that the moment of inertia is consistent with the presence of a substantial

* Corresponding author at: Department of Earth Sciences, University College London, Gower Street, London WC1E 6BT, UK. Tel.: +442076792383.
E-mail address: andrew.fortes@ucl.ac.uk

0032-0633/$ - see front matter © 2011 Elsevier Ltd. All rights reserved.
doi:10.1016/j.pss.2011.04.010

layer of hydrous silicates. Wholly undifferentiated models lead to MoI ≈ 0.39 (e.g., Zharkov et al., 1985; Fortes, 2004), and these might be attributed to an extremely slow accretionary process in which radiogenic heating from short-lived isotopes is negligible. Whilst it is intriguing that the models of Fortes et al. (2007) and Castillo-Rogez and Lunine (2010) yield MoI very close to that found by analysis of the Cassini data, we must nonetheless explore a broader range of chemically plausible parameter space so as to better interpret the gravity field observations. Iess et al. (2010) described the observed MoI as being "most reasonably … interpreted as a mixture of rock and ice (in the core)", whilst not excluding the possibility of a core composed of hydrous silicates. However, they presented no calculations to support these assertions, or to aid reproducibility of the interpretation by others. The objective of this work is to provide a suite of structural models – constructed with the minimum of model-dependent assumptions – in order to interpret the observed MoI of Titan.

2. Structural models of Titan's interior

I have constructed a broad suite of structural models using a finely laminated onion-skin model, the formulation of which is described elsewhere (Fortes, 2004). These models employ fully *P*,*T*-dependent equations of state for the constituent materials where available, and appropriate approximations in other cases. Densities as a function of pressure (depth) and temperature are calculated using a simple Murnaghan equation of state:

$$\frac{\rho_{0,T}}{\rho_{P,T}} = \left(1 + P\frac{K'}{K_T}\right)^{1/K'} \quad (1)$$

where $\rho_{0,T}$ is the density at $P=0$ and temperature T, $\rho_{P,T}$ is the density at pressure P and temperature T, K_T is the isothermal bulk modulus (=incompressibility) at $P=0$ and temperature T, and K' is the first pressure derivative of the bulk modulus, $(\partial K/\partial P)$. Density as a function of temperature at ambient pressure is found from either a temperature independent thermal expansivity, α, or from the expression below:

$$\rho_{0,T} = \rho_{0,0}\exp\left[-\left(\frac{A}{B+1}\right)T^{B+1}\right] \quad (2)$$

The bulk modulus is described by a polynomial of the form,

$$K_T = K_0 + CT + DT^2 \quad (3)$$

The first pressure derivative of the bulk modulus, K', is taken to be independent of temperature.

The equation of state parameters ρ_0, A, and B (or α), K_0, C, D, and K' for each material are reported in Table 1. These are derived either from single literature sources at reference P–T conditions, or have been obtained by fitting to many experimental data sets; pressure–volume–temperature data, melting volumes, and ultrasonic measurements. The parameters have been chosen to yield the best agreement with experimentally observed density values at pressure and temperature, and the greatest error is approximately 2% (see Fortes, 2004). The parameters for ice Ih have been updated to agree with the equation of state published by Feistel and Wagner (2006). The parameters of ice II have been modified to reflect new data obtained by the author (Fortes et al., 2009). For the generic 'rock' component, the thermoelastic properties were assumed to vary linearly as a function of density between the olivine and antigorite end-members, which is a sufficient approximation for these purposes.

Temperature profiles were imposed, rather than being calculated from heat flow models. Surface temperatures were pegged at 93 K and the central temperature at 900 K. In the thermal boundary layers at the top of the ice shell and the rocky core, thermal gradients of 8 K km^{-1} were used, with gradients of 0.1 K km^{-1} elsewhere (adapted after Grasset et al., 2000). In fact the structural models are comparatively insensitive to the temperature profile; the pressure is considerably more important.

I have constructed a range of static structural models and used Eq. (4) to compute the moment of inertia corresponding to each density profile. The *mean* moment of inertia, I, normalized by MR^2, for a given radial density profile, $\rho(r)$ is

$$\frac{I}{MR^2} = \frac{8}{3}\frac{\pi}{MR^2}\int_0^R \rho(r) r^4 \, dr \quad (4)$$

For slowly rotating bodies, where the difference in radius along the principal axes is very small, then the assumption that $I/MR^2 = C/MR^2$ is reasonable: the difference between the smallest and largest

Table 1
Equation of state parameters used in modelling the internal structure of Titan (see Fortes, 2004 and Section 2 for the origin of these values).

	Ice I	Ice V[a]	CH_4–clathrate I	San Carlos Olivine[b]	Liquid $Fe_{75}S_{25}$[c]
ρ_0(kg m^{-3})	934.31	1267.0	964.7	3343	4400
α (K^{-1})	–	4.50×10^{-5}	–	2.66×10^{-5}	1.10×10^{-4}
A	3.348×10^{-8}	–	7.77×10^{-8}	–	–
B	1.559	–	1.5578	–	–
K_0 (GPa)	10.995	13.93	10.025	131.1	12.5
C	−0.004068	–	−0.00407	−0.0223	−0.0104
D	-2.051×10^{-5}	–	-2.0513×10^{-5}	–	–
K'	7.000	5.20	5.2	3.8	5.5
	Ice II	**Ice VI**	**CH_4–clathrate II**	**Antigorite[b]**	**Solid iron[d]**
ρ_0 (kg m^{-3})	1199.65	1326.8	990	2558	7874
α (K^{-1})	–	–	–	2.00×10^{-5}	1.12×10^{-5}
A	1.027×10^{-6}	3.408×10^{-7}	–	–	–
B	1.005	1.2796	–	–	–
K_0 (GPa)	13.951	17.82	16.0	67.27	166.4
C	0.0014	−0.0385	–	−0.01	–
D	-4.25×10^{-5}	3.625×10^{-5}	–	–	–
K'	5.50	5.40	5.2	4.0	5.29

[a] P_{ref}=0.48 GPa, T_{ref}=237.65 K.
[b] T_{ref}=300 K.
[c] T_{ref}=1520 K.
[d] T_{ref}=300 K.

axial moments of inertia, A/MR^2 and C/MR^2, respectively, is simply J_2, which for Titan is approximately three parts in 10^5.

MoI have been computed for wholly undifferentiated structures (uniform mixtures of rock and ice), and fully differentiated structures (ice shells overlying rocky cores). I have also investigated means of *increasing* the density contrast from surface to core (i.e., smaller MoI) by introducing denser metallic inner cores, as well as means of *reducing* the density contrast (i.e., larger MoI) by mixing ice into the silicate core. In all instances, the models are constrained only by the observed radius and density of Titan; the adjustable parameters are therefore the radius of the major density discontinuity (the rock–ice interface) and the zero-pressure (uncompressed) density of the rocky core, which I take to be a proxy for the mineralogy of the core.

3. Results

3.1. Wholly undifferentiated and wholly differentiated models

The uppermost dashed line in Fig. 1 shows the MoI of an undifferentiated Titan in which rock and ice are mixed together uniformly from surface to core. The circles denote the rock mass fraction required for a given silicate density in order to be consistent with Titan's bulk density. In these models, the ice component experiences significant self compression and polymorphic transformation, including phases Ih, II, V, VI, and VII. The three solid lines at smaller MoI on Fig. 1 depict fully differentiated models of Titan. The middle black line represents a two-layer structure with a pure water-ice shell (phases Ih, II, V, and VI—see Table 2 for shell thicknesses and mean densities) overlying a silicate core. Circles indicate the core radius necessary for a given uncompressed rock density to yield the correct bulk density. It is suspected, on the basis of Cassini Radar observations which constrain the spin state (Lorenz et al., 2008), and on the detection of a Schumann resonance in Huygens Permittivity,

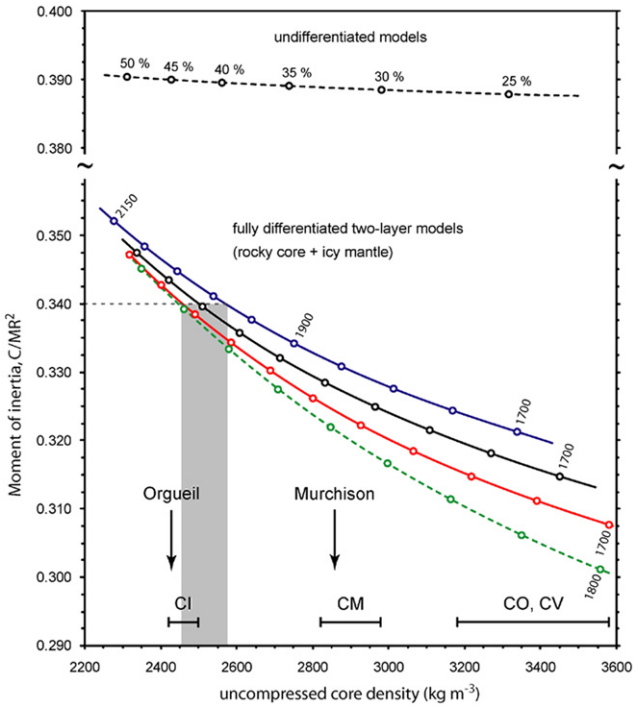

Fig. 1. Calculated moment of inertia for a suite of undifferentiated structures (upper dashed line) and a range of differentiated two-layer structures (lower solid and dashed lines—see Section 3.1 for details. The grey band depicts the range of silicate densities compatible with the observed MoI of Titan for differentiated structures with variable ice-mantle chemistry.

Table 2
Properties of a baseline two-layer structural model (ice shell over rocky core) consistent with the observed radius and mass of Titan, and MoI≡0.34.

Shell composition	Radius/shell thickness (km)	Mean density (kg m^{-3})	Mass ratio (%)
'Rock' core	2054	2584.1	69.7
Ice VI shell	132	1346.0	7.5
Ice V shell	117	1268.7	7.0
Ice II shell	125	1193.3	7.8
Ice Ih shell	146	932.8	8.0
Rock–ice interface pressure = 0.871 GPa			
Central pressure = 4.900 GPa			
Radioisotope	*Mass*	*Power*	
^{40}K	5.816×10^{15} kg	2.094×10^{11} W	
^{232}Th	2.898×10^{15} kg	7.826×10^{10} W	
^{238}U	7.879×10^{14} kg	7.485×10^{10} W	
Total		**3.625×10^{11} W**	**$=9.987 \times 10^{-9}$ W m^{-3}**

Isotopic abundances are derived from the observed abundances in CI chondrites (Lodders, 2003; De Laeter et al., 2003). Further example structures are given in Table 3.

Wave and Altimetry (PWA) data (Béghin et al., 2009, 2010), that Titan possesses a global subsurface ocean – perhaps at depths as shallow as 50 km – and I have therefore investigated the possible role that ocean chemistry (and hence density) may have on the calculated MoI. The lower solid red line represents a differentiated model in which a low-density liquid layer (zero-pressure $\rho = 950$ kg m^{-3}) of depth 250 km has been placed in the upper mantle beneath a 100 km-thick shell of ice Ih. The upper solid blue line represents a similar model in which a high-density liquid layer (zero-pressure $\rho = 1200$ kg m^{-3}) of depth 250 km lies beneath a 100 km-thick shell of ice Ih. These two extremes represent the likely lower and upper limits of plausible subsurface ocean densities, respectively, the lowest being close to the peritectic density of a water–methanol mixture (Yergovich et al., 1971; cf. Deschamps et al., 2010), and the highest being close to the eutectic density of a water–ammonium sulphate mixture (Novotný and Söhnel, 1988). Peritectic ammonia–water liquid (Croft et al., 1988) would fall on the low-density side of the solid-ice model (between the black and red solid lines). Oceans with an uncompressed density < 950 kg m^{-3} are gravitationally unstable with respect to the overlying ice shell, and oceans with an uncompressed density > 1200 kg m^{-3} are gravitationally unstable with respect to the underlying layer of ice VI. Finally, the dashed green line represents a model in which the shell of water ice is replaced entirely with solid methane clathrate consisting of the cubic structure-I phase to pressures of 0.7 GPa, and the marginally denser hexagonal structure-H phase at higher pressures. Clearly, for all physically plausible ocean chemistries, the range of admissible core densities for differentiated models with MoI≡0.34 is quite narrow; for the water-ice models (with and without oceans), the uncompressed silicate density is in the range 2463–2571 kg m^{-3}, corresponding to core radii of 2116–1984 km, respectively. For the methane clathrate model, MoI≡0.34 yields an uncompressed silicate density of 2448 kg m^{-3} and a core radius of 2157 km (Table 3). Reducing the possible MoI to 0.33 increases the allowed uncompressed density of the core and doubles the range to 2696–2910 kg m^{-3} (radii 1998–1838 km, respectively) for the water ice + ocean models, and 2653 kg m^{-3} (radius = 2072 km) for the solid clathrate model.

There are two possible interpretations of the low core density required by MoI ≈ 34; the first is that Titan's core consists of relatively low-density silicate minerals, and the second – described in the following subsection – is that the core comprises a mixture of denser silicate minerals with water ice.

Table 3
Properties of selected structural models of Titan's interior with MoI = 0.34.

	Methane clathrate model			**Pure water-ice model**			**Light-ocean (ρ_0 = 950 kg m^{-3})**			**Dense-ocean (ρ_0 = 1200 kg m^{-3})**		
	Depth/ radius (km)	Mean density (kg m^{-3})	Mass ratio (%)	Depth/ radius (km)	Mean density (kg m^{-3})	Mass ratio (%)	Depth/ radius (km)	Mean density (kg m^{-3})	Mass ratio (%)	Depth/ radius (km)	Mean density (kg m^{-3})	Mass ratio (%)
Ice Ih	–	–	–	146	932.8	8.0	100	930.9	5.6	100	930.9	5.6
MH-I	418	962.4	21.1	–	–	–	–	–	–	–	–	–
Ocean	–	–	–	–	–	–	250	1023.5	13.2	250	1281.3	16.5
Ice II	–	–	–	125	1193.3	7.8	–	–	–	–	–	–
Ice V	–	–	–	117	1268.7	7.0	62	1272.7	3.5	–	–	–
Ice VI	–	–	–	132	1346.0	7.5	47	1338.9	2.7	241	1350.9	13.4
'Rock'	2157	2525.3	78.9	2054	2584.1	69.7	2116	2542.3	75.0	1984	2650.4	64.5
$Fe_{75}S_{25}(l)$	–	–	–	–	–	–	–	–	–	–	–	–
$Fe(s)$	–	–	–	–	–	–	–	–	–	–	–	–
Rock–ice P (GPa)		0.574			0.871			0.702			1.041	
Rock-metal P (GPa)		–			––			–			–	
Core P (GPa)		4.829			4.900			4.850			4.987	

	Iron sulphide inner core			**Pure iron inner core**		
	Depth/radius (km)	Mean density (kg m^{-3})	Mass ratio (%)	Depth/radius (km)	Mean density (kg m^{-3})	Mass ratio (%)
Ice Ih	146	932.8	8.0	146	932.8	8.0
Ice II	125	1193.2	7.8	125	1193.2	7.8
Ice V	117	1268.6	7.0	117	1268.6	7.0
Ice VI	112	1344.5	6.4	116	1344.8	6.4
'Rock'	1775	2536.9	70.4	1771	2536.6	70.2
$Fe_{75}S_{25}(l)$	300	5541.2	0.5	–	–	–
$Fe(s)$	–	–	–	300	8058.3	0.7
Rock–ice P (GPa)		0.829			0.838	
Rock-metal P (GPa)		4.875			5.010	
Core P (GPa)		5.262			5.827	

Grain densities for CI, CM, CV, and CO carbonaceous chondrites are indicated in Fig. 1, as are the grain densities of the well-known Orgeuil (CI) and Murchison (CM) meteorites (Flynn et al., 1999; Consolmagno et al., 2008). The uncompressed core densities implied by MoI = 0.34 partially overlap with the measured grain densities of CI carbonaceous chondrites, which might suggest a similar mineralogy (Bland et al., 2004). Indeed, MoI = 0.342 is consistent with a slightly lower core density, which overlaps with the full range of CI chondrite grain densities, including Orgueil. The low density of CI chondrites is due to the presence of highly hydrated silicate phases, such as serpentine-group minerals (e.g., antigorite, lizardite) and smectite clays (e.g., saponite, nontronite), abundant sulphates and organic solids, with relatively small quantities of anhydrous silicates, oxides, and sulphides compared to other chondrite groups. If Titan's rocky core were to be mineralogically dominated by serpentine-group minerals then this has important consequences for the thermal structure, as discussed in Section 4, since these minerals experience a strongly endothermic dehydration reaction at comparatively modest temperatures (e.g., Wunder and Schreyer, 1997; Angel et al., 2001). *In situ* experimental studies of hydrothermal reactions in multi-phase chondritic systems at modest pressures and temperatures report the onset of antigorite dehydration, and the transformation of soluble organic carbon and sulphate to insoluble carbonate and sulphide at temperatures of ~700 K at 1.5 GPa (Scott et al., 2002).

3.2. Partially differentiated models

I have considered models in which the core is only partially differentiated, with the objective of determining whether Titan's MoI might be consistent with denser *anhydrous* silicates mixed with ice. The suite of models depicted in Fig. 2a and b consists of an outermost clean water-ice shell, an innermost ice-free silicate core, and an intermediate zone with a rock to ice ratio of 50:50 by mass. The solid lines in Fig. 2a show the radius of the inner ice-free core as a function of rock density (the lowermost cut-off being the fully differentiated model in Fig. 1). The solid lines in Fig. 2b report the same results in terms of the fractional core mass which is ice-free. For example, when only 20 wt% of the core remains ice-free (i.e., the outermost 80 wt% is a rock–ice mixture), then MoI = 0.34 is compatible with an uncompressed silicate density of ~3000 kg m^{-3}. The latter density is similar to the grain density of typical CM chondrites (Flynn et al., 1999: Consolmagno et al., 2008) and is more typical of the density of anhydrous silicate minerals. However, these models require substantially lower core temperatures than is the case even for a hydrated CI chondrite mineralogy, as dictated by the pressure melting curve of ice. For a model structure where ice VII is mixed to within 1200 km of Titan's core (equivalent to a mixed rock + ice zone ~ 900 km deep), the melting point at the inner-core interface (hydrostatic pressure = 3.37 GPa) is 443 K.

So, regardless of whether we choose to achieve Titan's low core density with CI chondritic rock, or with a mixture of CM (or denser) chondritic rock + ice, the core temperature must be many hundreds of degrees cooler than predicted in most previous models.

3.3. Metallic inner cores

Finally, I have investigated whether Titan could have a metallic inner core. Fig. 3 shows the MoI for a range of three-layer models in which a water-ice shell overlies a silicate outer core and a metallic inner core. Two extremes of plausible inner-core density have been modelled; Fig. 3a depicts the variation of MoI for a core of liquid $Fe_{75}S_{25}$ (approximately the low-pressure eutectic in the Fe–FeS system), which has a density of ~5500 kg m^{-3}, and Fig. 3b shows the variation of MoI for solid iron cores (density ~8000 kg m^{-3}).

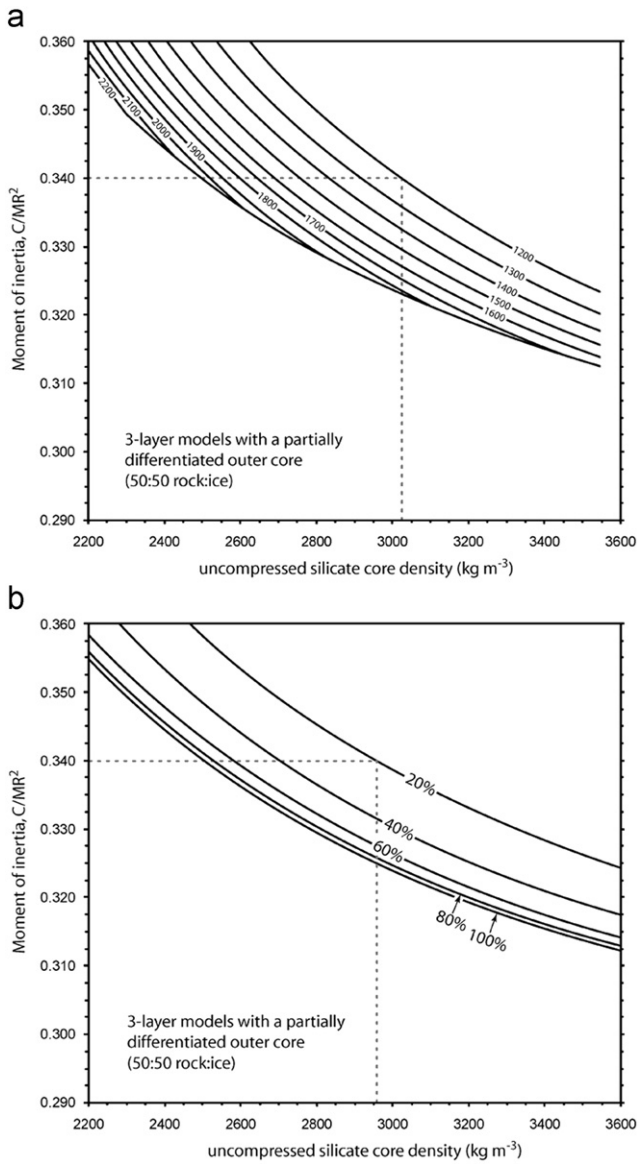

Fig. 2. Calculated moments of inertia for a suite of partially differentiated three-layer structures, consisting of an ice shell, a zone of mixed rock and ice, and an ice-free innermost core. The upper panel depicts the contours of inner core radius as a function of rock density and MoI, whereas the lower panel depicts the same information with inner-core volume as a fraction of the whole-core volume.

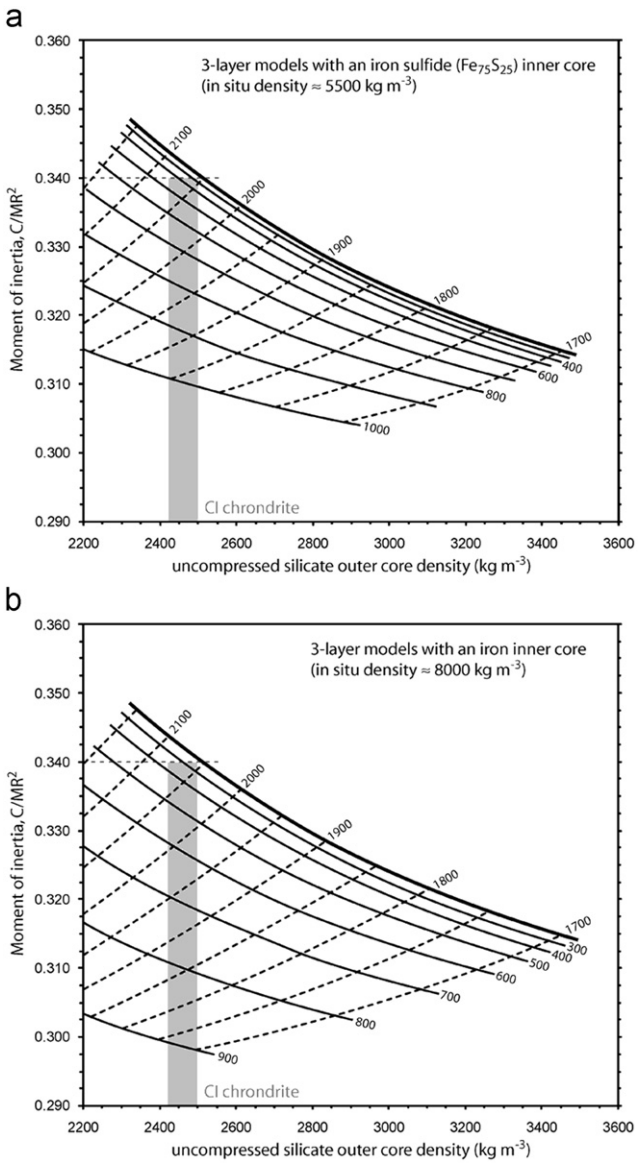

Fig. 3. Calculated moments of inertia for a suite of differentiated three-layer structures, consisting of an ice shell, a rocky outer core, and either an iron-sulphide inner core (a), or a pure iron inner core (b). The grey band depicts the range of CI carbonaceous chondrite grain densities, indicating the range of inner core radii, which may be compatible with MoI = 0.34.

Solid lines indicate the radius of the inner core, and dashed lines the radius to the rock–ice interface. The heavy solid lines represent the case from Fig. 1 where there is no metallic inner core. Clearly, for a given MoI, the addition of any denser metallic material in the centre of Titan requires a lower-density mantle, either from lower density silicates, or a greater admixture of ice. The vertical grey bar depicts the range of CI chondrite grain densities: if we assume that the silicate portion of the core has a CI mineralogy, then MoI = 0.34 is consistent with a liquid $Fe_{75}S_{25}$ inner core of radius 358^{+80}_{-140} km, or a solid iron inner core of radius 287^{+68}_{-125} km. In fact, the MoI is relatively insensitive to iron cores with radii smaller than ~200 km so the lower size limit for this rock density, in both cases, is essentially zero. Adopting the marginally larger observed MoI = 0.342 reduces the *upper limit* on the allowed radius of a possible metallic core (with a CI chondrite mantle) to 320 km ($Fe_{75}S_{25}$) and 215 km (Fe), respectively. Given that smaller rock (or rock + ice) densities are indicative of core temperatures too low to allow partial melting and segregation of metal into an inner core, then the balance of probability must be that MoI = 0.34 means that Titan has no metallic core, although formally I cannot exclude metallic cores with radii of a few hundred kilometres: such small cores represent a very small fraction of Titan's total mass (< 0.5 wt%). The lack of an observed intrinsic magnetic field at Titan (Ness et al., 1981, 1982; Backes et al., 2005) is not necessarily a useful constraint, since an inner core may be entirely solidified, or may be entirely liquid (e.g., Grasset et al., 2000) but convecting very weakly or not at all.

4. Discussion

The presence today of a low-density core (Fig. 4) – whatever its nature – suggests that Titan accreted sufficiently slowly for heating by short-lived isotopes, such as ^{26}Al, to be insignificant. As stated earlier, either case places limits on the present day temperature of the core, these limits being more strict in the case of a rock–ice core (~450 K) than the case of a serpentinite core

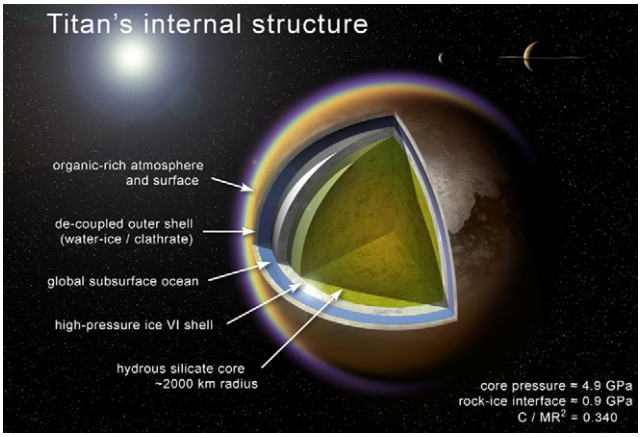

Fig. 4. Scale illustration of one possible fully differentiated internal structure model for Titan, in which the core consists entirely of hydrous silicates and an ocean of liquid water exists in the upper part of the ice mantle.

(700–900 K). Iess et al. (2010) drew attention to the latter but not the former in their brief discussion of the matter; it is not obvious why they preferred a partially differentiated structure since it would appear more difficult in that case to keep Titan's core sufficiently cool.

If Titan's core consists largely of hydrous silicates, then the core presumably became hydrated in the manner attributed to the CI chondrite parent body—by hydrothermal convection after the completion of differentiation (cf., Travis and Schubert, 2005); it is well known that the serpentinization process creates microfractures, which allow fluid migration even under high hydrostatic pressures. Grindrod et al. (2008) computed a range of thermal evolutionary paths for Titan models containing a serpentinized core: these models used a higher volumetric power due to radiogenic decay of long-lived isotopes than we would expect from a large CI chondrite-like core (1.61×10^{8} W m^{-3} vs. 1.00×10^{8} W m^{-3}; see Table 2), and obtained temperature increases of ~300 K over 4.5 Ga. We must bear in mind that potassium is very soluble; significant quantities of ^{40}K may be leached from the core and subsequently become concentrated in a subsurface ocean, leaving only uranium and thorium as major sources of core heating. Hence the volumetric power in Table 2 is likely to be an upper limit. In order to preserve the temperature of Titan's core *below* the dehydration temperature of the proposed constituent hydrous silicates then we require temperatures at the close of accretion to be ~500 K (or ~100 K to keep a rock–ice core below the melting point of constituent ices). However, the process of de-watering the core (either by dehydration of hydrous silicates or melting of occluded high-pressure ice) is not instantaneous since each has a significant (and indeed comparable) phase transition enthalpy, which acts to damp any further heating whilst the reaction progresses. Grindrod et al. (2008) did not consider the dehydration enthalpy of hydrous silicates in their calculation of Titan's thermal evolution after the dehydration temperature was reached. The dehydration of serpentinite is a strongly endothermic reaction, with enthalpies in the range of ~370 J g^{-1} for antigorite, to ~565 J g^{-1} for lizardite (values at 100 kPa, see Weber and Greer, 1965). The ability of serpentinites to absorb heat is a familiar problem to geologists modelling the penetration of a pervasively hydrated slab of oceanic crust into the mantle at subduction zones (e.g., Anderson et al., 1978). Adopting the conservative value of the dehydration enthalpy, $\Delta H=250$ J g^{-1}, as used in terrestrial slab de-watering models, it is obvious that were the core to reach the temperature at which dehydration commences, then there is sufficient energy available to dehydrate the entire core more than twice over in 4.5 Ga. This cannot have occurred or else the MoI would be considerably lower than 0.34, as clearly illustrated in Fig. 1. If, for example, the onset of dehydration commenced 500 million years ago, then up to 20 wt% of the core may have become completely de-watered (and much less if the core is depleted in ^{40}K). This corresponds to a relatively small reduction in the bulk density and the overall volume of the core (~5%), distributed either uniformly or in a shell ~100 km thick (possibly with active hydrothermal circulation) at the rock–ice interface. This condition is just on the high-density side of the grey band in Fig. 1, but likely to be admissible by the uncertainty in the MoI. Consequently, some degree of core dehydration may be underway *if* the dehydration temperature has been reached in the geologically recent past, with the outcome that superheated water will be driven into the overlying ice mantle; in turn this may initiate plume activity in the mantle with extensive resurfacing and outgassing as a possible result. This is essentially the state of affairs predicted by the recent model of Castillo-Rogez and Lunine (2010), and it is reassuring that these two independently derived models arrive at similar conclusions concerning the state of Titan's core.

Serpentinization by CO_2-bearing fluids can produce methane and heavier hydrocarbons; this mechanism has been mooted as an endogenic source for Titan's atmospheric methane (Zolotov et al., 2005; Atreya et al., 2006; Guo and Eiler, 2007). Both methane clathrate and heavier liquid alkanes are buoyant with respect to all of the ice polymorphs likely to comprise Titan's mantle, and these may act as a means of delivering organic chemicals to the near-surface environment. Subsequent dissociation of the clathrate species to liberate the guest gases is problematic since either a very large thermal anomaly is required, contact with a liquid in which the clathrate is unstable (Choukroun et al., 2010 proposed concentrated ammonia-water liquid), or a smaller degree of heating combined with a reduction in pressure (Fortes et al., 2007 proposed entrainment of clathrate xenoliths in a cryovolcanic liquid). The ^{12}C/^{13}C ratio in methane near the surface of Titan is 91.1 ± 1.4 (Niemann et al., 2010), which is close to the solar value: superficially, this might be taken to mean that methane was accreted directly into Titan as methane clathrate. However, there are uncertainties concerning the possible fractionation of carbon isotopes by any of the proposed methane synthesis mechanisms (note that both biotic *and* abiotic methane synthesis mechanisms, including serpentinization, yield isotopically light carbon), and the subsequent outgassing to the atmosphere, and no conclusion may be drawn from the measured ^{12}C/^{13}C ratio (see Atreya et al., 2006 for a further discussion). Recently, the inferred D/H ratio of the proto-Saturnian water reservoir has been used to conclude that methane in Titan's atmosphere cannot have been produced by serpentinization of silicates in the core, although these models do not rule out the occurrence of serpentinization, only placing limits on the oxidation state of putative hydrothermal systems (Glein et al., 2009; Mousis et al., 2009).

Gases produced in the core are likely to interact with high-pressure ices at the base of the mantle to form clathrate hydrates. Clathrates of both Ar and CH_4 have been synthesized at high-pressure (at room temperature) by Ogienko et al. (2006); the structure H[1] clathrate of Ar was formed at 760 MPa, presumably by direct reaction with ice VI, after a period of a few weeks, and the structure II clathrate of CH_4 was formed at 500 MPa. At the base of Titan's ice mantle (pressure ~900 MPa) we would expect to form, respectively, the tetragonal clathrate of Ar (Manakov et al., 2004) and the structure H clathrate of CH_4. Unfortunately, very little information exists concerning the diffusion of gas species through either

[1] Refer to Fortes and Choukroun (2010) for a discussion of clathrate structure types.

low- or high-pressure forms of ice, or through the structures of clathrate hydrates. Experimental measurements are difficult, and the computational tools necessary to calculate diffusivities and activation energy barriers are only recently becoming tractable to use (e.g., Ammann et al., 2010). Molecular dynamics calculations (using interatomic potentials) show that Ar can infiltrate the structure of ice II, whereupon further diffusion is halted (Malenkov and Zheligovskaya, 2004). This work also shows that there is no diffusion of Ar in the structure II Ar clathrate. Similar calculations with CO_2 show a 100-fold reduction in the diffusivity (at the same temperature) between ice Ih and the structure I clathrate (cf. Demurov et al., 2002 with Ikeda-Fukuzawa et al., 2004). However, CO_2 is a linear molecule and can pass more readily than CH_4 through the ring structures in the clathrate structure. The most advanced calculations to date (*ab initio* density functional theory+van der Waals) by Román-Pérez et al. (2010) show that the barrier to passage of CH_4 through the hexagonal rings of the structure I clathrate is 40 times greater than for a linear molecule such as H_2, requiring a "substantial relaxation" of the host structure: the passage of CH_4 through the pentagonal rings destroys the clathrate structure. Clearly, experiments reveal that clathrates of both Ar and CH_4 will form rapidly under the conditions of Titan's lower mantle, but calculations suggest that further diffusion of these species is reduced either by orders of magnitude or stopped entirely, effectively capping any further escape of these gases. Unless these clathrates are carried to the surface – perhaps by large-scale mantle convection – and subsequently dissociated, then we should not be surprised if there is only the most limited gas exchange between the core and the surface.

5. Summary

Titan's observed moment of inertia strongly indicates that the satellite's rocky core is of a lower density than expected, either as a result of being highly hydrated, or due to a significant admixture of ice. Both cases constrain the interior to be much cooler than previously anticipated, which calls into question the interpretation of Titan's endogenic surface activity. A cool partially differentiated interior is no impediment to the existence of a subsurface ocean, as demonstrated by Callisto, although none of these data place constraints on the composition of any subsurface ocean.

Titan's internal structure appears to differ from other icy solar system objects of similar dimensions. Callisto's MoI (0.3549 ± 0.0042) indicates a largely undifferentiated structure (Anderson et al., 2001). Ganymede's MoI (0.3105 ± 0.0028), in combination with detection of an intrinsic magnetic field, is consistent with the presence of a liquid metallic core and a silicate mantle of density 3300 kg m^{-3} overlain by an ice shell (Anderson et al., 1996). Titan may be no more "Callisto with weather" (Moore and Pappalardo, 2011) than it is like Ganymede without a metal core; it is possibly a quite different – more organic-rich – object. Further modelling of Titan's interior is required to reconcile a cool core with the observed level of apparently endogenic surface modification (Lunine et al., 2008) and to ensure that this is consistent with the structural constraints implied by Titan's orbital eccentricity. It is also important to understand any chemical and isotopic fractionation mechanisms which may occur as hydrothermally generated gases (and radiogenic gases) make their way towards the surface, whether by molecular diffusion or by enclathration and subsequent dissociation. These results may have significance for the possible organic chemistry of the ice shell, the composition and thermal balance of any subsurface ocean, and the astrobiological potential of Titan as a whole (Norman and Fortes, 2011). Future landed missions to Titan's surface (e.g., Coustenis and et al., 2009) should carry seismometers capable of detecting the interface between the ice shell and the rocky core as well as possible upper and lower boundaries of a subsurface ocean.

Acknowledgments

ADF is funded by a STFC Advanced Fellowship (PP/E006515/1). The author thanks Luciano Iess for useful discussions concerning the Cassini gravity data, and two anonymous reviewers for helping to improve the manuscript.

References

Ammann, M.W., Brodholt, J.P., Dobson, D.P., 2010. Simulating diffusion. In: Theoretical and computational methods in mineral physics: geophysical applications. Rev. Min. Geochem. 71, 201–224.
Anderson, J.L., Jacobson., R.A., McElrath, T.P., Moore, W.B., Schubert, G., Thomas, P.C., 2001. Shape, mean radius, gravity field, and interior structure of Callisto. Icarus 153 (1), 157–161.
Anderson, J.L., Lau, E.L., Sjogren, W.L., Schubert, G., Moore, W.B., 1996. Gravitational constraints on the internal structure of Ganymede. Nature 384, 541–543.
Anderson, R.J., DeLong, S.E., Schwarz, W.M., 1978. Thermal model for subduction with dehydration in the downgoing slab. J. Geol. 86 (6), 731–739.
Angel, R.J., Frost, D.J., Ross, N.L., Hemley, R., 2001. Stabilities and equations of state of dense hydrous magnesium silicates. Phys. Earth. Planet. Int. 127, 181–196.
Atreya, S.K., Adams, E.Y., Niemann, H.B., Demick-Montelara, J.E., Owen, T.C., Fulchignoni, M., Ferri, F., Wilson, E.H., 2006. Titan's methane cycle. Planet. Space. Sci. 54 (12), 1177–1187.
Backes, H., Neubauer, F.M., Dougherty, M.K., Achilleos, N., André, N., Arridge, C.S., Bertucci, C., Jones, G.H., Khurana, K.K., Russell, C.T., Wennmacher, A., 2005. Titan's magnetic field signature during the first Cassini encounter. Science 308, 992–995.
Béghin, C., Canu, P., Karkoschka, E., Sotin, C., Bertucci, C., Kurth, W.S., Berthelier, J.J., Grard, R., Hamelin, M., Schwingenschuh, K., Simões, F., 2009. New insights on Titan's plasma-driven Schumann resonance inferred from Huygens and Cassini data. Planet. Space Sci. 57 (14–15), 1872–1888.
Béghin, C., Sotin, C., Hamelin, H., 2010. Titan's native ocean revealed beneath some 45 km of ice by a Schumann-like resonance. Comptes Rendus Geosci. 342 (6), 425–433.
Bland, P.A., Cressey, G., Menzies, O.N., 2004. Modal mineralogy of carbonaceous chondrites by X-ray diffraction and Mössbauer spectroscopy. Meteoritics Planet. Sci. 39 (1), 3–16.
Castillo-Rogez, J.C., Lunine, J.I., 2010. Evolution of Titan's rocky core constrained by Cassini observations. Geophys. Res. Lett. 37 article L20205.
Choukroun, M., Grasset, O., Tobie, G., Sotin, C., 2010. Stability of methane clathrate hydrates under pressure: influence on outgassing processes of methane on Titan. Icarus 205 (2), 581–593.
Consolmagno, G.J., Britt, D.T., Macke, R.J., 2008. The significance of meteorite density and porosity. Chemie der Erde 68, 1–29.
Coustenis, A., 154 co-authors, 2009. TandEM; Titan and Enceladus mission. Exp. Astron. 23 (3), 893–946.
Croft, S.K., Lunine, J.I., Kargel, J.S., 1988. Equation of state of ammonia-water liquid—derivation and planetological applications. Icarus 73 (2), 279–293.
De Laeter, J.R., Böhlke, J.K., de Bièvre, P., Hidaka, H., Peiser, H.S., Rosman, K.J.R., Taylor, P.D.P., 2003. Atomic weights of the elements. Pure Appl. Chem. 75 (6), 683–800.
Demurov, A., Radhakrishnan, R., Trout, B.L., 2002. Computations of diffusivities in ice and CO_2 clathrate hydrates via molecular dynamics and Monte Carlo simulations. J. Chem. Phys. 116 (2), 702–709.
Deschamps, F., Mousis, O., Sanchez-Valle, C., Lunine, J.I., 2010. The role of methanol in the crystallization of Titan's primordial ocean. Astrophys. J. 724 (2), 887–894.
Elliot, J.L., Veverka, J., Goguen, J., 1975. Lunar occultation of Saturn I—the diameters of Tethys, Dione, Rhea, Titan, and Iapetus. Icarus 26, 387–407.
Feistel, R., Wagner, W., 2006. A new equation of state for H_2O ice Ih. J. Chem. Ref. Data 35 (2), 1021–1047.
Flynn, G.J., Moore, L.B., Klöck, W., 1999. Density and porosity of stone meteorites: implications for the density, porosity, craterings, and collisional disruption of asteroids. Icarus 142 (1), 97–105.
Fortes, A. (2004) Computational and experimental studies of solids in the ammonia–water system. Ph.D. Thesis, University of London.
Fortes, A.D., Grindrod, P.M., Trickett, S.K., Vočadlo, L., 2007. Ammonium sulfate on Titan: possible origin and role in cryovolcanism. Icarus 188 (1), 139–153.
Fortes, A.D., Wood, I.G., Vočadlo, L., Knight, K.S., Marshall, W.G., Tucker, M.G., Fernandez-Alonso, F., 2009. Phase behaviour and thermoelastic properties of perdeuterated ammonia hydrate and ice polymorphs from 0 to 2 GPa. J. Appl. Cryst. 42 (5), 846–866.
Fortes, A.D., Choukroun, M., 2010. Phase behaviour of ices and hydrates. Space Sci. Rev. 153 (1–4), 185–218.
Glein, C.R., Desch, S.J., Shock, E.L., 2009. The absence of endogenic methane of Titan and its implications for the origin of atmospheric nitrogen. Icarus 204 (2), 637–644.
Grasset, O., Sotin, C., Dechamps, F., 2000. On the internal structure and dynamics of Titan. Planet. Space Sci. 48 (7–8), 617–636.

Grindrod, P.M., Fortes, A.D., Nimmo, F., Feltham, D.L., Brodholt, J.P., Vočadlo, L., 2008. The long-term stability of a possible aqueous ammonium sulfate ocean inside Titan. Icarus 197 (1), 137–151.
Guo, W., Eiler, J.M., 2007. Temperatures of aqueous alteration and evidence for methane generation on the parent bodies of the CM chondrites. Geochim. Cosmochim. Acta 71 (22), 5565–5575.
Iess, L., Rappaport, N.J., Jacobson, R., Racioppa, P., Stevenson, D.J., Armstrong, J.W., Asmar, S.W., Tortora, P., 2010. Gravity field, shape and moment of inertia of Titan. Science 327, 1367–1369.
Ikeda-Fukuzawa, T., Kawamura, K., Hondoh, T., 2004. Mechanism of molecular diffusion in ice crystals. Mol. Simul. 30 (13–15), 973–979.
Jacobson, R.A., Antreasian, P.G., Bordi, J.J., Criddle, K.E., Ionasescu, R., Jones, J.B., Mackenzie, R.A., Meek, M.C., Parcher, D., Pelletier, F.J., Owen Jr., W.M., Roth, D.C., Roundhill, I.M., Stauch, J.R., 2006. The gravity field of the Saturnian system from satellite observations and spacecraft tracking data. Astron. J. 132 (6), 2520–2526.
Lodders, K., 2003. Solar system abundances and condensation temperatures of the elements. Astrophys. J. 591 (2), 1220–1247.
Lorenz, R.D., Stiles, B.W., Kirk, R.L., Allison, M.D., del Marmo, P.P., Iess, L., Lunine, J.I., Ostro, S.J., Hensley, S., 2008. Titan's rotation reveals an internal ocean and changing zonal winds. Science 319, 1649–1651.
Lunine, J.I., 43 co-authors, 2008. Titan's diverse landscapes as evidenced by Cassini RADAR's third and fourth looks at Titan. Icarus 195 (1), 415–433.
Lupo, M.J., 1982. Mass–radius relationships in icy satellites after Voyager. Icarus 52 (1), 40–53.
Lupo, M.J., Lewis, J.S., 1979. Mass–radius relationships in icy satellites. Icarus 40 (2), 157–170.
Malenkov, G.G., Zheligovskaya, E.A., 2004. Dynamics of some He and Ar clathrate hydrates. Computer simulation study. J. Incl. Comp. Macrocycl. Chem. 48, 45–54.
Manakov, A.Yu., Voronin, V.I., Kurnosov, A.V., Teplykh, A.E., Larionov, E.G., Dyadin, Yu.A., 2004. Argon hydrates: structural studies at high pressures. Dokl. Phys. Chem. 378 (4–6), 148–151.
Moore, J.M., Pappalardo, R.T., 2011. Titan, an exogenic world? Icarus 212 (2), 790–806.
Mousis, O., Lunine, J.I., Pasek, M., Cordier, D., Waite, J.H., Mandt, K.E., Lewis, W.S., Nguyen, M.–J., 2009. A primordial origin for the atmospheric methane of Saturn's moon Titan. Icarus 204 (2), 749–751.
Murray, C.D., Dermott, S.F., 1999. Solar System Dynamics. Cambridge University Press.
Ness, N.F., Acuña, M.H., Behannon, K.W., Burlaga, L.F., Connerney, J.E.P., Lepping, R.P., Neubauer, F.M., 1982. Magnetic field studies by Voyager 2—preliminary results at Saturn. Science 215, 558–563.
Ness, N.F., Acuña, M.H., Lepping, R.P., Connerney, J.E.P., Behannon, K.W., Burlaga, L.F., Neubauer, F.M., 1981. Magnetic field studies by Voyager 1—preliminary results at Saturn. Science 212, 211–217.
Niemann, H.B., Atreya, S.K., Demick, J.E., Gautier, D., Haberman, J.A., Harpold, D.N., Kasprzak, W.T., Lunine, J.I., Owen, T.C., and Raulin, F. (2010): Composition of Titan's lower atmosphere and simple surface volatiles as measured by the Cassini–Huygens probe gas chromatograph mass spectrometer experiment. J. Geophys. Res. – Planets 115 article E1 2006.
Norman, L.H., Fortes, A.D., 2011. Is there life on Titan? Astron. Geophys. 52 (1), 39–42.
Novotný, P., Söhnel, O., 1988. Densities of binary aqueous solutions of 306 inorganic substances. J. Chem. Eng. Data 33 (1), 49–55.
Ogienko, A.G., Kurnosov, A.V., Manakov, A.Y., Larionov, E.G., Ancharov, A.I., Sheromov, M.A., Nesterov, A.N., 2006. Gas hydrates of argon and methane synthesized at high pressures: composition, thermal expansion, and self-preservation. J. Phys. Chem. B 110, 2840–2846.
Prentice, A.J.R. (2007) Titan's physical and chemical structure: predictions for a capture origin. LPSC XXXVIII, abstract 2402.
Reynolds, R.T., Cassen, P.M., 1979. On the internal structure of the major satellites of the outer planets. Geophys. Res. Lett. 6 (2), 121–124.
Román-Pérez, G., Moiaed, M., Soler, J.M., & Yndurain, F. (2010) Stability, adsorption and diffusion of CH_4, CO_2 and H_2 in clathrate hydrates. Phys. Rev. Lett. 105. article 145901.
Schubert, G., Spohn, T., Reynolds, R.T., 1986. Thermal histories, compositions and internal structures of the moons of the solar system. In: Burns, J.A., Matthews, M.S. (Eds.), Satellites. University of Arizona, Tucson, AZ, pp. 224–292.
Scott, H.P., Williams, Q., Ryerson, F.J., 2002. Experimental constraints on the chemical evolution of large icy satellites. Earth Planet. Sci. Lett. 203 (1), 399–412.
See, T.J.J., 1902. Observations of the diameters of the satellites of Jupiter, and of Titan, the principal satellite of Saturn. Astron. Nachr. 157, 325–336.
Sohl, F., Hussmann, H., Scwentker, B., Spohn, T., Lorenz, R.D., 2003. Interior structure models and tidal Love numbers of Titan. J. Geophys. Res. 108 (E12) article 5130.
Sohl, F., Sears, W.D., Lorenz, R.D., 1995. Tidal dissipation on Titan. Icarus 115 (2), 278–294.
Tobie, G., Grasset, O., Lunine, J.I., Mocquet, A., Sotin, C., 2005. Titan's internal structure inferred from a coupled thermal-orbital model. Icarus 175 (2), 496–502.
Tobie, G., Lunine, J.I., Sotin, C., 2006. Episodic outgassing as the origin of atmospheric methane on Titan. Nature 440, 61–64.
Travis, B.J., Schubert, G., 2005. Hydrothermal convection in carbonaceous chondrite parent bodies. Earth Planet. Sci. Lett. 240 (2), 234–250.
Weber, J.N., Greer, R.T., 1965. Dehydration of serpentine: heat of reaction and reaction kinetics at $P_{H_2O} = 1$ atm. Am. Mineral. 50, 450–464.
Wunder, B., Schreyer, W., 1997. Antigorite: high-pressure stability in the system $MgO–SiO_2–H_2O$ (MSH). Lithos 41 (1–3), 213–227.
Yergovich, T.W., Swift, G.W., Kurata, F., 1971. Density and viscosity of aqueous solutions of methanol and acetone from the freezing point to 10 °C. J. Chem. Eng. Data 16 (2), 222–226.
Zharkov, V.N., Leontjev, V.V., Kozenko, A.V., 1985. Models, figures, and gravitational moments of the Galilean satellites of Jupiter and icy satellites of Saturn. Icarus 61 (1), 92–100.
Zolotov, M.Y., Owen, T., Atreya, S., Niemann, H.B., Shock, E.L., 2005. An endogenic origin of Titan's methane. American Geophysical Union, Fall Meeting, abstract P43B-04.